

Effect of mild baking on superconducting niobium cavities investigated by sequential nanoremoval

A. Romanenko,* A. Grassellino, and F. L. Barkov

Fermi National Accelerator Laboratory, Batavia, IL 60510, USA

J. P. Ozelis

Facility for Rare Isotope Beams, East Lansing, MI 48824, USA

(Dated: August 22, 2012)

Abstract

Near-surface nanostructure of niobium determines the performance of superconducting microwave cavities. Subtle variations in surface nanostructure lead to yet unexplained phenomena such as the dependence of the quality factor of these resonating structures on the magnitude of RF fields - an effect known as the “Q-slopes”. Understanding and controlling the Q-slopes is of great practical importance for particle accelerators. Here we investigate the mild baking effect - 120°C vacuum baking for 48 hours - which strongly affects the Q-slopes. We used a hydrofluoric acid rinse alternating with oxidation in water as a tool for stepwise material removal of about 2 nanometers/step from the surface of superconducting niobium cavities. Applying removal cycles on mild baked cavities and measuring the quality factor dependence on the RF fields after one or several such cycles allowed us to explore the distribution of lossy layers within the first several tens of nanometers from the surface. We found that a single HF rinse results in the increase of the cavity quality factor. The low field Q-slope was shown to be mostly controlled by the material structure within first 6 nanometers from the surface. The medium field Q-slope evolution was fitted using linear ($\propto H$ peak surface magnetic field) and quadratic ($\propto H^2$) terms in the surface resistance and it was found that best fits do not require the quadratic term. We measured that about 10 nanometers of material removal are required to bring back the high field Q-slope and about 20-50 nanometers to restore the onset field to the pre-baking value.

* aroman@fnal.gov

I. INTRODUCTION

The quality factor of superconducting niobium cavities exhibits a field dependence characterized by three distinct regions in the $Q_0(H_{\text{peak}})$ curve (see Ref. 1 for review). Underlying mechanisms, which govern these so-called *Q-slopes*, are not clear despite a number of studies in the recent decade. One of the major obstacles is the absence of a full nanoscale understanding of the material changes in the magnetic field penetration depth ($\lesssim 100$ nm) brought about by different treatments applied on cavities. Such treatments include electropolishing (EP), buffered chemical polishing (BCP), 120°C baking, and 600-800°C baking in vacuum furnaces.

While there are no established methods to control low and medium field Q-slopes, it was discovered that the high field Q-slope (HFQS) can be removed by a so-called *mild baking* - an in situ ultra high vacuum annealing of cavities at 90-145°C for the duration of 12-48 hours. In addition to the removal of the HFQS, mild baking was demonstrated to lead to a decrease in BCS surface resistance by up to $\sim 50\%$ and to an increase in the residual resistance. What the material-level mechanism is, which underlies the mild baking effect, remains the main unresolved issue. Several important clues were obtained by cavity experiments. First, by oxipolishing experiments the change in BCS surface resistance after 145°C 45 hours bake was found to extend down to about 300 nanometers from the surface [2]. Second, it was demonstrated by cavity anodizing experiments [3, 4] that modifications introduced by mild baking at 100-120°C, which are affecting the high field Q-slope, are confined to only ~ 20 -30 nanometers from the surface.

While anodizing studies provided an indication of the crucial length scales for the mild baking effect on the high field Q-slope, it is important to study in detail how all of the Q-slopes (and not only HFQS) evolve when baking-modified material is being removed. Such detailed information is important for understanding how surface nanostructure leads to the particular low, medium, and high field Q-slopes and to provide experimental data for models to compare against. Furthermore, anodizing process involves electric potential and oxygen diffusion, which potentially may play a role in the observed changes. Thus using a different method of nanoremoval serves as an independent cross-check of the anodizing results.

In this article we report measurements on the cavities where as a means of nanoremoval we utilized a hydrofluoric acid (48% concentrated) rinse for 5 minutes followed by several

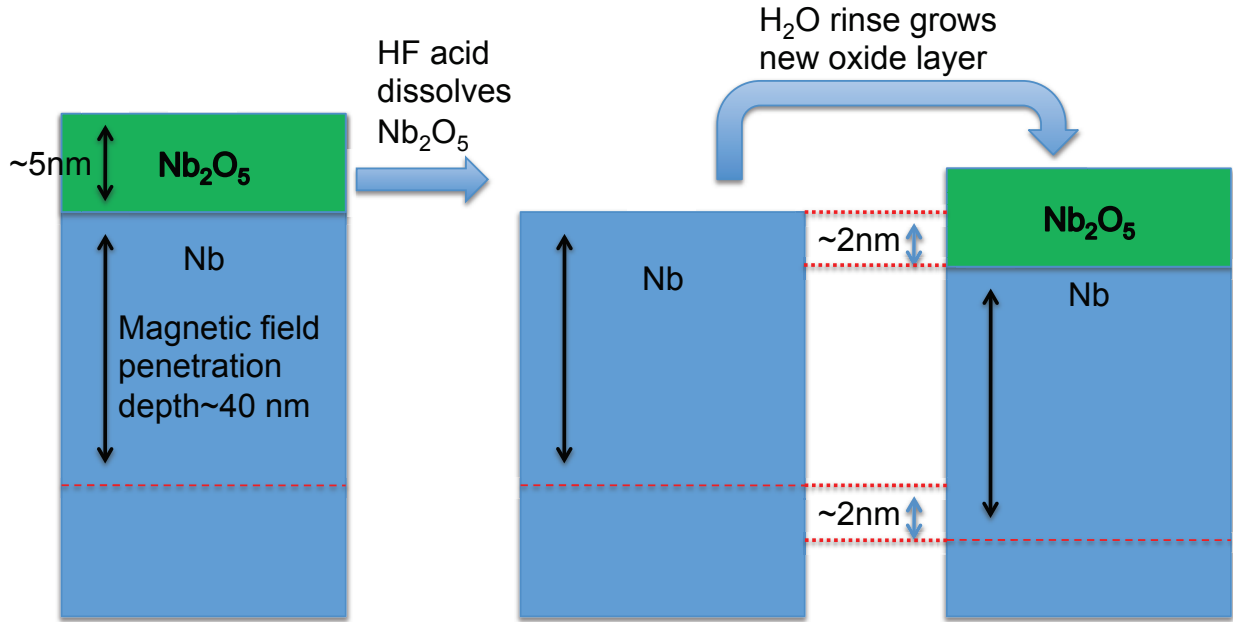


FIG. 1. Schematic of the nanoremoval during a single HF/water rinse cycle.

ultrapure water rinses. Typically HF rinse is used in SRF field to remove a pentoxide layer, i.e. a thick oxide formed by anodizing in oxipolishing. The oxide layer is then regrown upon air or water exposure. We assume the following sequence in our experiments: 1) HF rinse removes the niobium pentoxide (Nb_2O_5) layer; 2) air exposure/water rinse regrows a new Nb_2O_5 layer of 4-5 nanometers thick. Forming 4-5 nanometers of pentoxide consumes about 1.5-2 nanometers of niobium as estimated from the corresponding densities. Hence the net effect of a single HF rinse cycle is to regrow a new wet oxide and push the layer with RF currents deeper by about 1.5-2 nanometers. Schematic sequence of events during such treatment is shown in Fig. 1. The primary difference of such process from anodizing is the absence of electric potential. A possible side effect of HF rinsing (as well as oxipolishing used in Ref. 2) may be due to entering of hydrogen into niobium whenever the protective Nb_2O_5 layer is not present.

We report RF measurements after nanoremoval steps of the quality factor versus temperature, from which we extract how superconducting parameters change as a function of depth, and $Q_0(H_{\text{peak}})$ curves, which provide information on the change in Q-slopes.

II. EXPERIMENTAL

Three different 1.3 GHz niobium cavities of TESLA elliptical shape were used for these studies. Niobium properties and surface treatments that were applied on cavities are summarized in Table I.

TABLE I. List of cavities used for experiments.

Cavity ID	Material	Manufacturer	Treatment
TE1ACC002	RRR \gtrsim 200, grain size \sim 50 μ m	ACCEL	Bulk EP + tumbling + light EP
TE1ACC005	RRR \gtrsim 200, grain size \sim 50 μ m	ACCEL	Bulk EP
TE1AES003	RRR \gtrsim 200, grain size \sim 50 μ m	AES	Bulk BCP

Before the series of HF rinses each of the cavities was baked at 120°C for 48 hours in vacuum. As expected, it removed the high field Q-slope in EP cavities TE1ACC002 and TE1ACC005 while only shifting it to slightly higher fields in the BCP cavity TE1AES003.

After each rinsing cycle(s) we measured the cavity quality factor Q_0 at 2 K as a function of the accelerating gradient E_{acc} . In some tests additional measurements of $Q_0(T)$ at $E_{\text{acc}} = 5$ MV/m in the temperature range $1.5 < T < 2$ K were performed. For TESLA elliptical geometry the ratio of peak surface magnetic field H_{peak} to E_{acc} is 4.26 mT/(MV/m) and for convenience all test results are plotted as $Q_0(H_{\text{peak}})$. All RF measurements at 2 K for three different cavities we used are presented in Fig. 2-4.

To visualize better the evolution of shapes of $Q_0(H_{\text{peak}})$ curves, plots of $Q_0/Q_{\text{max}}(H_{\text{peak}})$, where Q_{max} is the maximum quality factor in each case, are shown in Fig. 5.

III. DISCUSSION

A. Evolution of residual and BCS resistances

It is important to understand how effective values of the residual and BCS surface resistances, superconducting gap, and electron mean free path vary in mild baking cavities with distance from the surface. We can semi-quantitatively extract such values from fits to the temperature dependence of the quality factor $Q_0(T)$ measured after each HF rinse cycle.

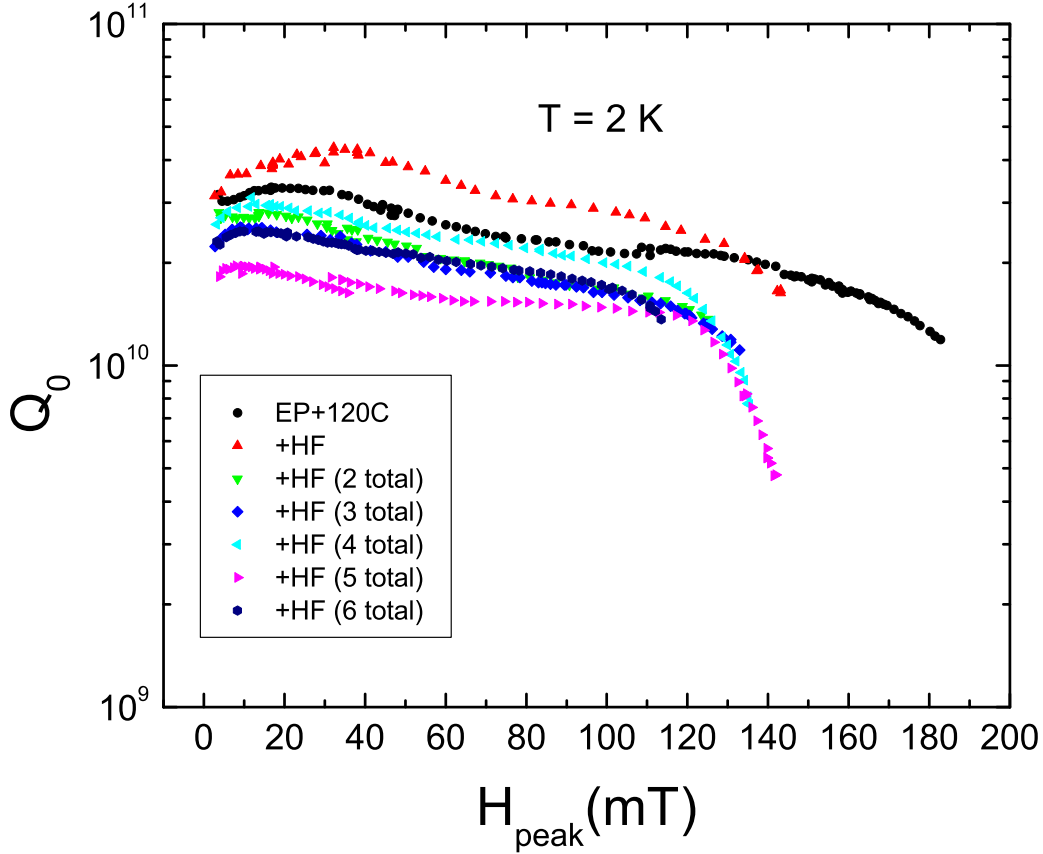


FIG. 2. Cavity RF test results after multiple HF rinse cycles for the electropolished tumbled cavity TE1ACC002.

This information can help in understanding what the underlying driving factors for the mild baking effect and Q-slopes are on the material level.

We have performed such measurements only on the electropolished tumbled cavity TE1ACC002 due to the technical constraints. In future experiments we plan to repeat $Q(T)$ measurements on other cavities prepared similarly to TE1ACC002. For TE1ACC002 we measured the temperature dependence $Q_0(T)$ at $E_{\text{acc}} = 5$ MV/m ($H_{\text{peak}} \approx 21$ mT) for $1.55 < T < 2$ K in all RF tests in addition to 2 K Q-curve. The average surface resistance calculated as $\bar{R}_s = G/Q_0$ where $G = 270$ is a geometry factor, is shown in Fig. 6 for data obtained after each of the HF rinses.

It is worth mentioning that since a fixed input coupler with the external quality factor of $Q_{\text{ext}} \sim 10^{10}$ was used in all RF tests, measurement errors are getting large as the Q_0

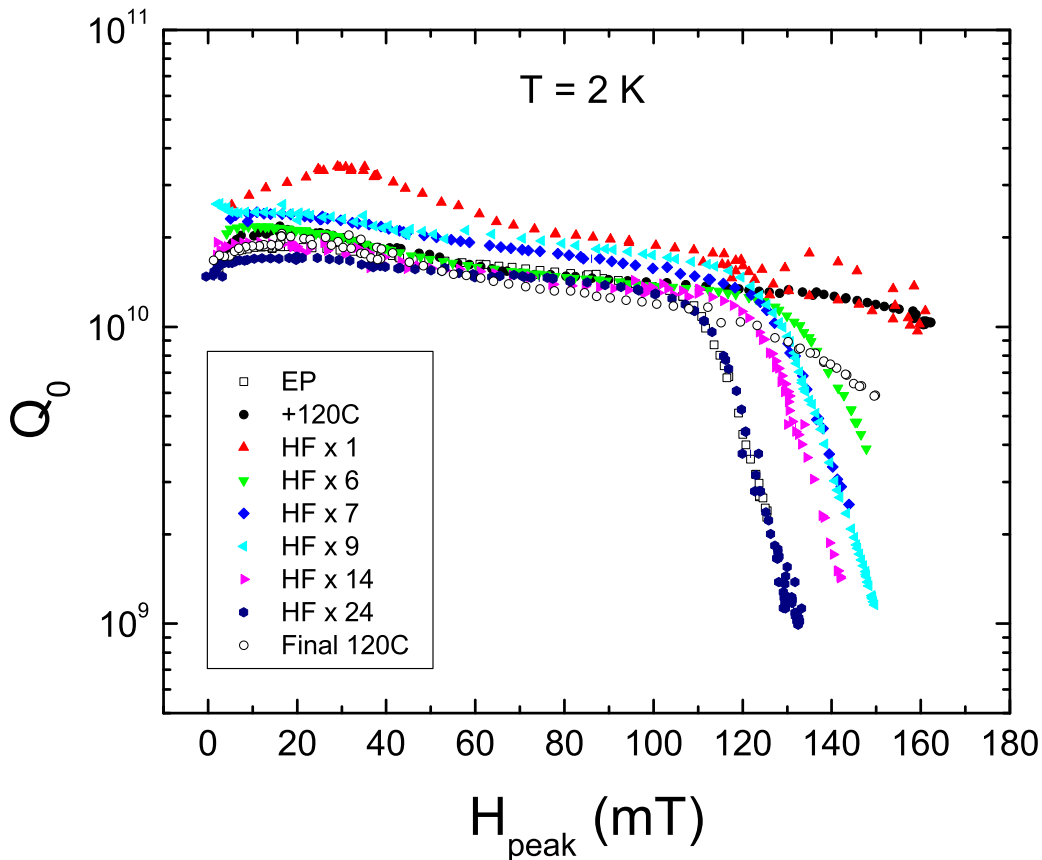


FIG. 3. Cavity RF test results after multiple HF rinse cycles for the electropolished cavity TE1ACC005. No field emission was present except for the final 120°C test.

increases beyond 5×10^{10} making the exact Q_0 measurement a challenge. Thus most of the results at lower temperatures with very high quality factors should be taken with caution providing a qualitative performance comparison rather than exact quantitative one.

We used the code [5] based on the original Halbritter's program [6] for weakly coupled BCS model with diffuse scattering to fit $R_s(T)$ with fixed parameters $T_c = 9.25$ K, $\lambda_0 = 30$ nm, $\xi_0 = 39$ nm, and varying free parameters - residual resistance R_{res} , superconducting gap $\Delta/(k_B T_c)$, and electron mean free path l_{mfp} . Fit results are summarized in Table II. It should be noted that BCS surface resistance is only weakly dependent on the electron mean free path within the temperature range we studied. As a consequence our extracted values of l_{mfp} suffer from a big uncertainty prohibiting any definitive conclusions regarding its evolution with HF rinses. On the other hand, the residual resistance can be extracted

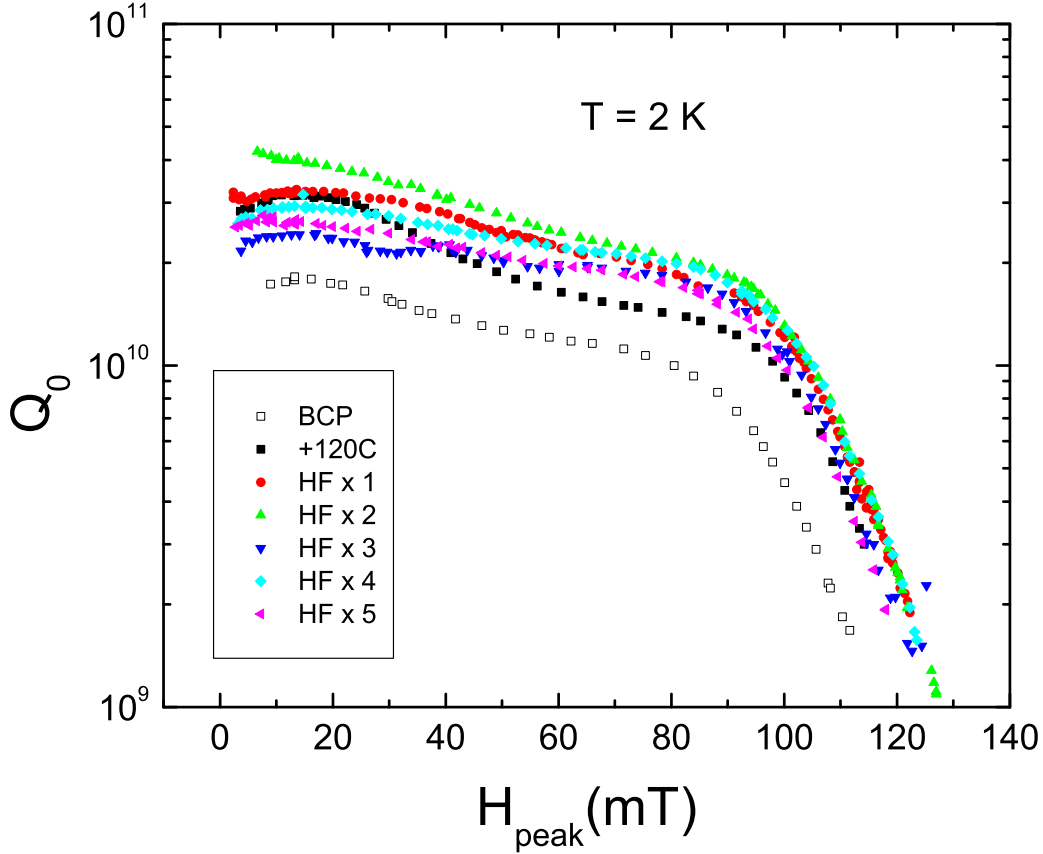


FIG. 4. Cavity RF test results after multiple HF rinse cycles for the buffered chemical polished cavity TE1AES003.

pretty accurately and hence both R_{res} and R_{BCS} are more reliable indicators of the changes.

We should comment on the negative residual resistance after a single HF rinse. Since the quality factor is very high ($> 4 \times 10^{10}$) even at 2 K and increasing rapidly upon cooldown, the error is large for most of the points in $Q_0(T)$ curve. Thus the negative residual resistance may be an artifact reflecting the low residual resistance value affected by the measurement error.

Our data show a gradual increase in BCS surface resistance with the depth of the material removed starting from the second HF rinse. Such an increase is consistent with the observations of Kneisel [2] and supports a gradual consumption of the lower mean free path layer by HF rinsing.

The residual resistance is decreased after a single HF rinse, which is followed by the

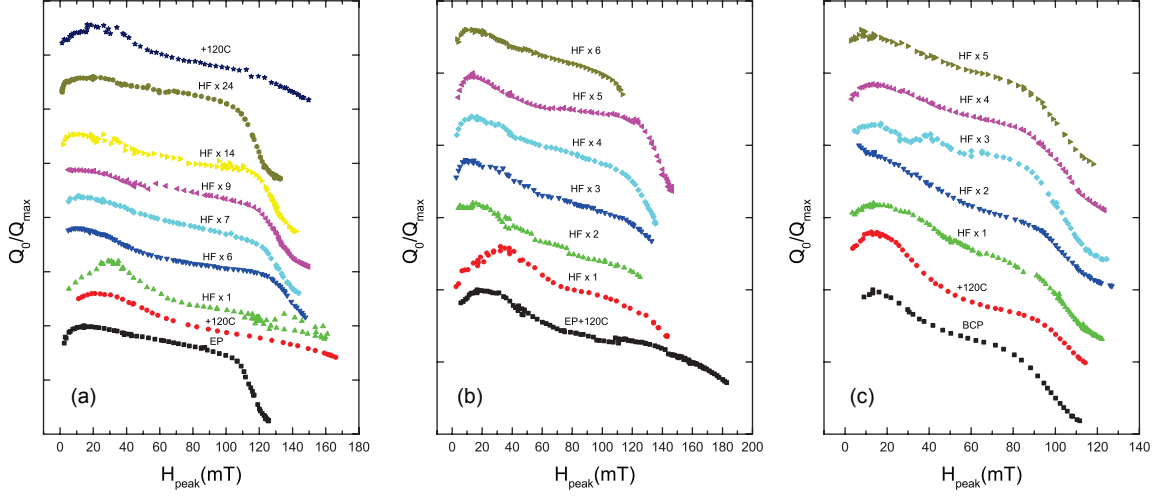


FIG. 5. Evolution of $Q_0(H_{\text{peak}})$ curve shapes with multiple HF rinse cycles for: (a) electropolished cavity TE1ACC005; (b) electropolished cavity TE1ACC002 with tumbling to a mirror smooth finish as one of the processing steps; (c) buffered chemical polished cavity TE1AES003.

TABLE II. Changes in the superconducting properties after HF rinsing cycles for the bulk EP tumbled cavity TE1ACC002.

Treatment	$R_{\text{res}}(\text{n}\Omega)$	$R_{\text{BCS}}(\text{n}\Omega)$	$\Delta/(kT_c)$	$l_{\text{mfp}}(\text{nm})$
EP + 120°C	1.3	7.2	1.84	26
HF rinse x 1	-0.4	7.1	1.86	26
HF rinse x 2	1.5	8.08	1.83	33
HF rinse x 3	2.8	8.31	1.81	38
HF rinse x 4	0.2	9.33	1.80	25
HF rinse x 5	3.9	9.53	1.80	27

increasing trend with subsequent rinses except for a rinse #4. Thus no systematic trend can be clearly observed after second and subsequent rinses.

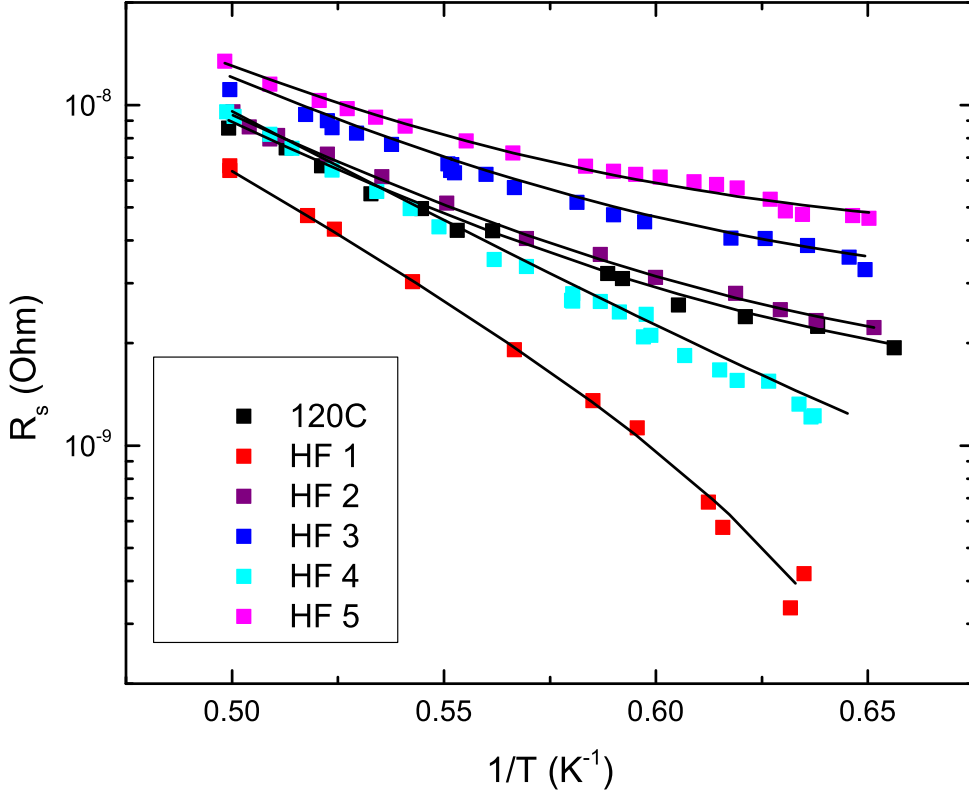


FIG. 6. Average surface resistance $R_s = G/Q_0$ at $H_{\text{peak}} \approx 21$ mT after multiple HF rinse cycles for the electropolished tumbled cavity TE1ACC002. Black lines represent fits to the data based on the weakly coupled BCS approximation using the code from [5].

B. Single HF rinse as a way of Q_0 maximization

One of the apparent effects observed on all three cavities is a significant increase in the quality factor at low and medium fields after a single HF rinse cycle. As mentioned above, mild baking has two side effects: a decrease in the BCS surface resistance R_{BCS} by a factor of up to 2, and an increase in the residual resistance R_{res} . Reversing an increase in R_{res} and keeping the benefit in R_{BCS} should allow minimizing the total surface resistance. We believe the observed Q_0 increase may stem from the decrease of the residual resistance by a single HF rinse consistent with earlier literature reports [4]. This means that the increase in

R_{res} caused by mild baking is due to the changes in either the oxide or in the first 1.5-2 nm of niobium underneath it. If it is due to oxide changes then it may be attributed to the formation of normal conducting NbO_x clusters or layer. If it is due to niobium underneath it may be caused by the interstitial oxygen enrichment.

It is worth noting that a very high quality factor $Q_0 > 2 \times 10^{11}$ at 1.6 K at low fields was measured in TE1ACC002 after the first HF rinse. This corresponds to a total surface resistance of order 1 nOhm. But due to the large errors caused by fixed coupler at high Q_0 values, this result should be taken with caution.

Many future accelerators are based on the superconducting RF technology and are intended to be operated in a CW regime. It makes the minimization of the RF losses at a moderate field level (i.e. 70 mT for Project X) a task of major importance since it directly translates into the costs associated with the required refrigeration power. Based on our findings, a single HF rinse performed after 120°C baking represents a simple technique to maximize low/medium field Q_0 with minimal modifications to the existing processing sequence.

C. Q-slopes

One of the main goals of our study is to get insight into what is responsible for different Q-slopes. In particular, one of the questions is where the particular features/layers leading to the low, medium and high field Q-slopes are localized with respect to the niobium surface. To answer this question we analyze in detail the evolution of each of the Q-slopes with HF treatments and extract possible depth distributions of the corresponding parameters.

1. Low field Q-slope

Low field Q-slope (LFQS) is typically observed as an increase in the cavity quality factor Q_0 with field in the range of surface magnetic fields of 0-20 mT. There is a very limited number of studies of this effect [7, 8] reported in the literature.

Several models have been put forward to explain the LFQS. One of the models is based on the presence of NbO_x clusters at the oxide-metal interface [9]. Another model relies on the presence of small weakly superconducting defects [10]. These models predict the inverse

quadratic dependence of the surface resistance on the peak magnetic field (although due to different mechanisms):

$$R_s = \frac{a}{H^2} + b \quad (1)$$

One more model is based on the hypothesis that niobium surface in a cavity can be treated as a two-layer superconductor with the “dirty” superconductor film on top of bulk niobium [11].

Low field Q-slope can be easily explained by additional field-independent dissipated power. In fact any dissipative mechanism, which leads to a dissipated power P_{diss} per unit area with the field dependence weaker than $\propto H^2$ will result in the low field Q-slope. Indeed, suppose we have additional losses $P^*(H)$. Then:

$$\begin{aligned} Q_0(H) &= \frac{\omega U}{P_{\text{diss}}} \propto \frac{\int_V H^2 dv}{\int_S R_s(H) H^2 ds + P^*(H)} \\ &\propto \frac{\text{const}}{\text{const} + P^*(H)/H^2} \Rightarrow R_s(H) \propto 1/Q_0(H) \\ &= \text{const} + \text{const} \cdot P^*(H)/H^2 \quad (2) \end{aligned}$$

which will be an increasing function of H if $P^*(H)$ has a weaker than H^2 character, leading to the low field Q-slope. In particular, if $P^*(H)=\text{const}$ then we recover a LFQS parametrization as in Eq. 1.

We find that Eq. 1 describes our data reasonably well with several important exceptions. This finding points toward the constant with field additional dissipated power behind the LFQS for most of the cases as explained above.

First exception is that LFQS in both TE1ACC002 and TE1ACC005 cavities after a single HF rinse could not be fitted with Eq. 1. Second exception is the absence of the low field Q-slope in both TE1ACC002 and TE1AES003 after two HF rinses. We have no explanation for these facts at the moment.

In Table III the values of the best fit parameters to our data based on Eq. 1 are presented. Corresponding plots of the best fit parameters as a function of approximate thickness of niobium consumed by HF rinsing cycles are shown in Fig. 7.

LFQS “strength” characterized by a appears to be significantly enhanced by 120°C treatment. It is suppressed by the next two HF rinses with the values appearing to remain at approximately the same average value after third and subsequent HF rinses. The constant b , which captures the variation of the surface resistance at the peak of the $Q_0(H)$ curve, exhibits lowest values after a single HF rinse followed by an upward trend with further HF

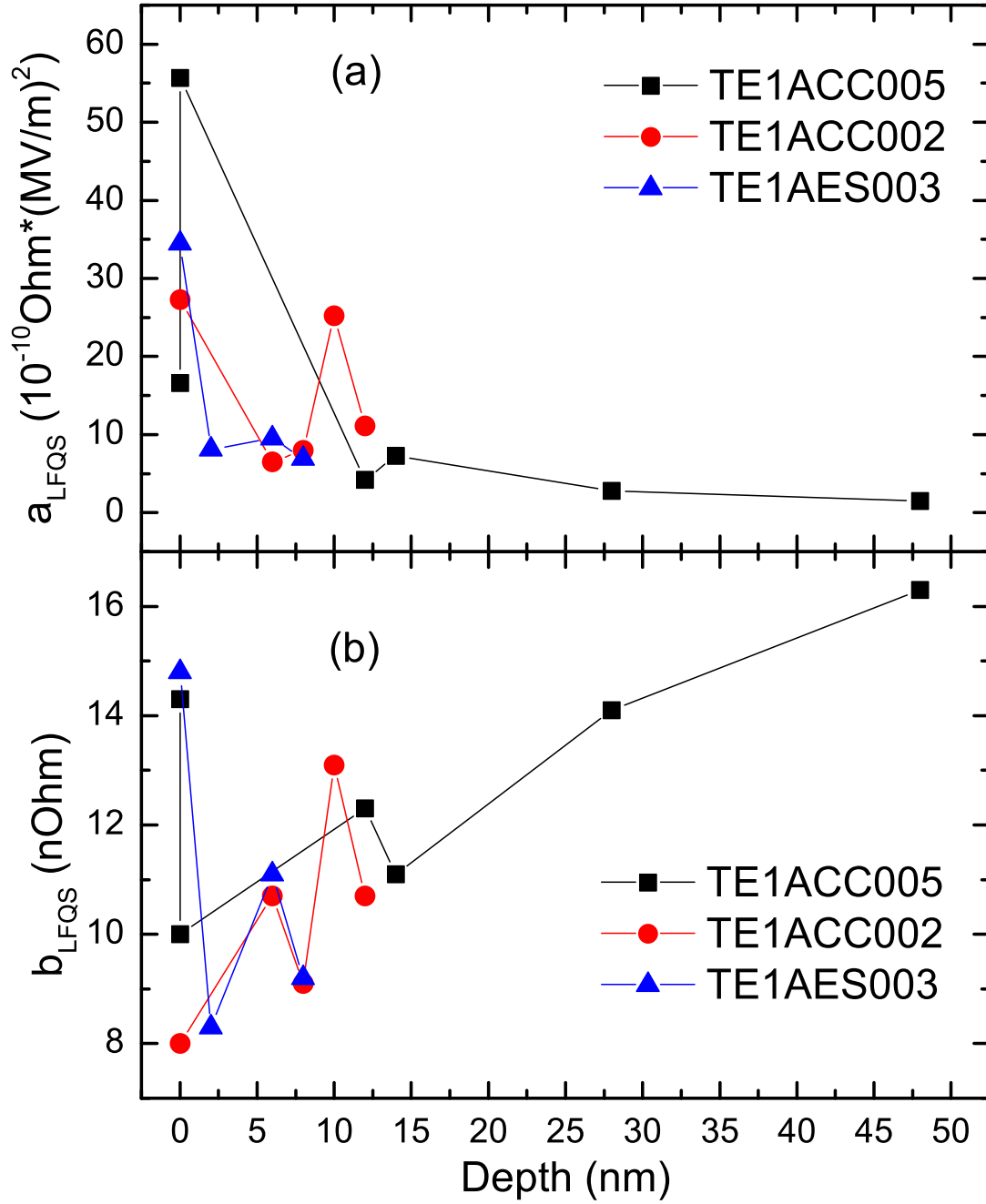


FIG. 7. LFQS fit results for parameters a and b as a function of material removal depth.

TABLE III. Parameters for the fits based on Eq. 1 of the low field Q-slope in the bulk electropolished (EP) cavity (TE1ACC005), bulk EP + tumbling + light EP cavity (TE1ACC002), and a buffered chemically polished (BCP) cavity (TE1AES003).

TE1ACC005	$a \cdot 10^{10}$	$b(nOhm)$	r^2
EP not baked	16.6	14.3	0.961
EP + 120°C	55.7	10.0	0.995
HF rinse x 1 ^a	-	-	-
HF rinse x 6	4.2	12.3	0.926
HF rinse x 7	7.3	11.1	0.745
HF rinse x 9 ^b	-	-	-
HF rinse x 14	2.8	14.1	0.954
HF rinse x 24	1.5	16.3	0.918
TE1ACC002			
EP + 120°C	27.3	8.0	0.934
HF rinse x 1 ^a	-	-	-
HF rinse x 2 ^b	-	-	-
HF rinse x 3	6.5	10.7	0.913
HF rinse x 4	8.0	9.1	0.974
HF rinse x 5	25.2	13.1	0.974
HF rinse x 6	11.1	10.7	0.997
TE1AES003			
BCP no bake	34.5	14.8	0.977
BCP + 120°C ^a	-	-	-
HF rinse x 1	8.1	8.3	0.977
HF rinse x 2 ^b	-	-	-
HF rinse x 3	9.5	11.1	0.904
HF rinse x 4	6.9	9.2	0.979
HF rinse x 5 ^c	-	-	-

^a Fit by Eq. 1 was not possible - a different field dependence is present.

^b No low field Q-slope was observed.

^c Too few points measured in the LFQS range.

rinses. Therefore, the low field Q-slope appears to be the very surface effect governed by the material within 3 HF rinses corresponding to about 4.5-6 nanometers from the surface.

2. Medium field Q-slope

Medium field Q-slope (MFQS) is a decrease in Q_0 with field over the peak magnetic field range of about 20-80 mT. Several mechanisms have been proposed to explain the effect. One of the mechanisms is based on the presence of normal conducting niobium hydrides, which would produce a linear dependence of extra surface resistance on H as found for the case of Q-disease [12]. Halbritter [13] proposed an additional term in the surface resistance coming from hysteretic losses caused by Josephson fluxons entering niobium at “strong” links such as oxidized grain boundaries. Losses due to such fluxons are proportional to the magnetic field H as well. Additionally, two separate quadratic in H terms were suggested to come from thermal feedback due to the exponential dependence of the BCS surface resistance on temperature [9], and due to the non-linear Meissner effect [14]. Weingarten [10] proposed small weakly superconducting defects at the surface of niobium as yet another possible source of the MFQS. Whichever model turns out to be correct should reflect the recently reported high magnetic field localization of the medium field losses [15].

For all of the models above the following parametrization of the surface resistance is typically used for fitting the $Q_0(H)$ dependence in the medium field range:

$$R_s = R_0 \left(1 + \gamma \left(\frac{H}{H_c} \right)^2 \right) + R_1 \left(\frac{H}{H_c} \right) \quad (3)$$

Using Eq. 3 for fits we found that quadratic component is not needed to fit our data. In Table IV values of the fit parameters providing the best fit (maximizing r^2) to our data are presented. Except for two cases when RF calibration problems were encountered during testing (footnoted in Table IV), the fits are excellent and describe well the medium field Q-slope. The change of the fit parameter R_1 with the approximate thickness of consumed niobium is shown in Fig. 8.

Two primary conclusions can be drawn from our data.

First, the slope-defining parameter R_1 is changing throughout the whole material removal sequence all the way down to 24 HF rinses corresponding to about 36-48 nm of niobium. That means that, unlike LFQS, the MFQS origin is not localized at the very surface but is

TABLE IV. Parameters for the fits based on Eq. 3 of the medium field Q-slope in the bulk electropolished (EP) cavity (TE1ACC005), bulk EP + tumbling + light EP cavity (TE1ACC002), and a buffered chemically polished (BCP) cavity (TE1AES003).

TE1ACC005	$R_0(nOhm)$	$R_1(nOhm)$	r^2
EP not baked	13.2	11.2	0.995
EP + 120°C	7.2	18.8	0.995
HF rinse x 1	4.1	23.2	0.988
HF rinse x 6	11.9	16.3	0.988
HF rinse x 7	9.9	13.9	0.996
HF rinse x 9	9.1	12.7	0.999
HF rinse x 14	12.7	16.9	0.986
HF rinse x 24	15.0	9.6	0.995
TE1ACC002			
EP + 120°C	6.2	13.8	0.982
HF rinse x 1	4.2	11.7	0.967
HF rinse x 2	7.7	17.6	0.981
HF rinse x 3	9.7	13.8	0.982
HF rinse x 4	8.5	9.7	0.984
HF rinse x 5	1.5	8.1	0.845 ^a
HF rinse x 6	10.1	10.6	0.989
TE1AES003			
BCP no bake	11.9	36.2	0.989
BCP + 120°C	4.0	41.8	0.998
HF rinse x 1	5.9	20.2	0.974
HF rinse x 2	4.8	20.0	0.992
HF rinse x 3	10.2	11.5	0.974
HF rinse x 4	7.7	15.1	0.993
HF rinse x 5	8.5	17.4	0.990

^a The fit is poor for this measurement due to the cable calibration problems during the RF test.

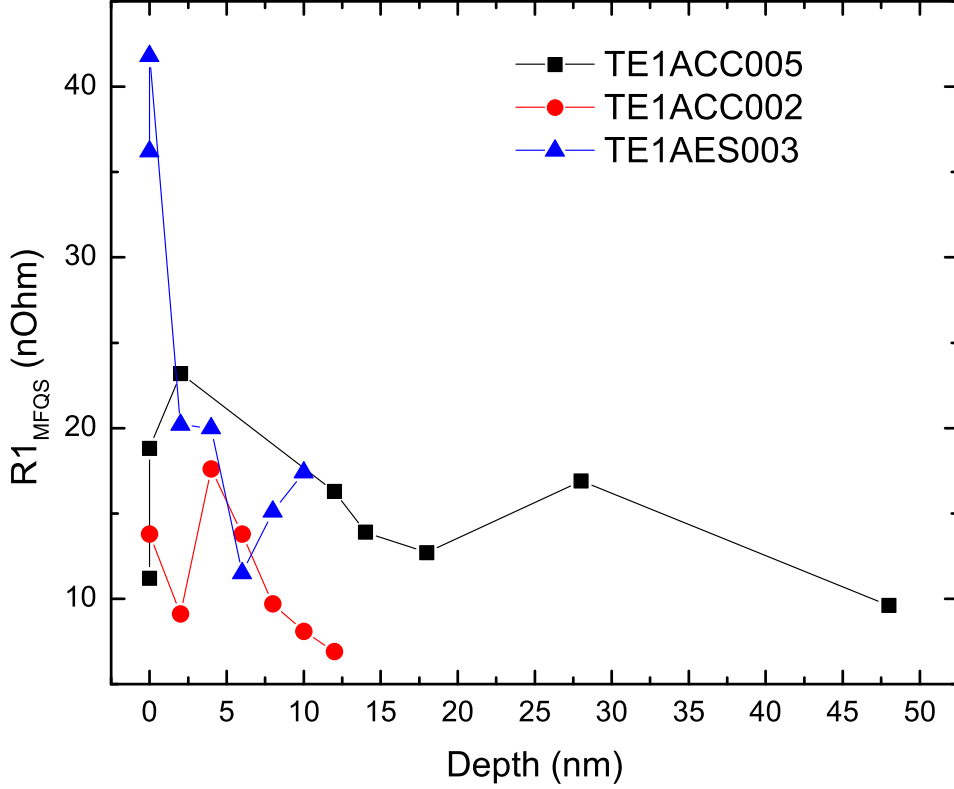


FIG. 8. MFQS fit results for the parameter R_1 with $\gamma = 0$ for all fits as a function of material removal depth.

residing within the larger thickness of several tens of nanometers.

Second, the fact that the quadratic term $\propto H^2$ in $R_s(H)$ is not required to fit our data indicates that suggested physical mechanisms based on the thermal feedback and non-linear Meissner effect are less probable. On the other hand, mechanisms leading to the linear term, among which are hydrides and oxidized strong links, are consistent with our observations.

3. High field Q -slope

The physical mechanism behind the *high field Q -slope* (HFQS) remains elusive despite the significant effort towards understanding this interesting phenomenon (see [16–18] for review). It was reported that a single HF rinse applied on mild baked cavities does not

bring the HFQS back [16] but there is no data in the literature for multiple HF rinse cycles. Anodizing experiments [3, 4] showed that when about 20-30 nm of niobium are converted to oxide the HFQS reappears. This thickness corresponds to about 10-15 HF rinses in our experiments.

In our data we observe a gradual high field Q-slope reappearance in both TE1ACC002 (tumbled EP) and TE1ACC005 (EP) cavities. To demonstrate this point a set of $\bar{R}_s = G/Q_0$ curves is shown for TE1ACC005 in Fig. 9. After 6 HF rinses (\approx 9-12 nm of niobium

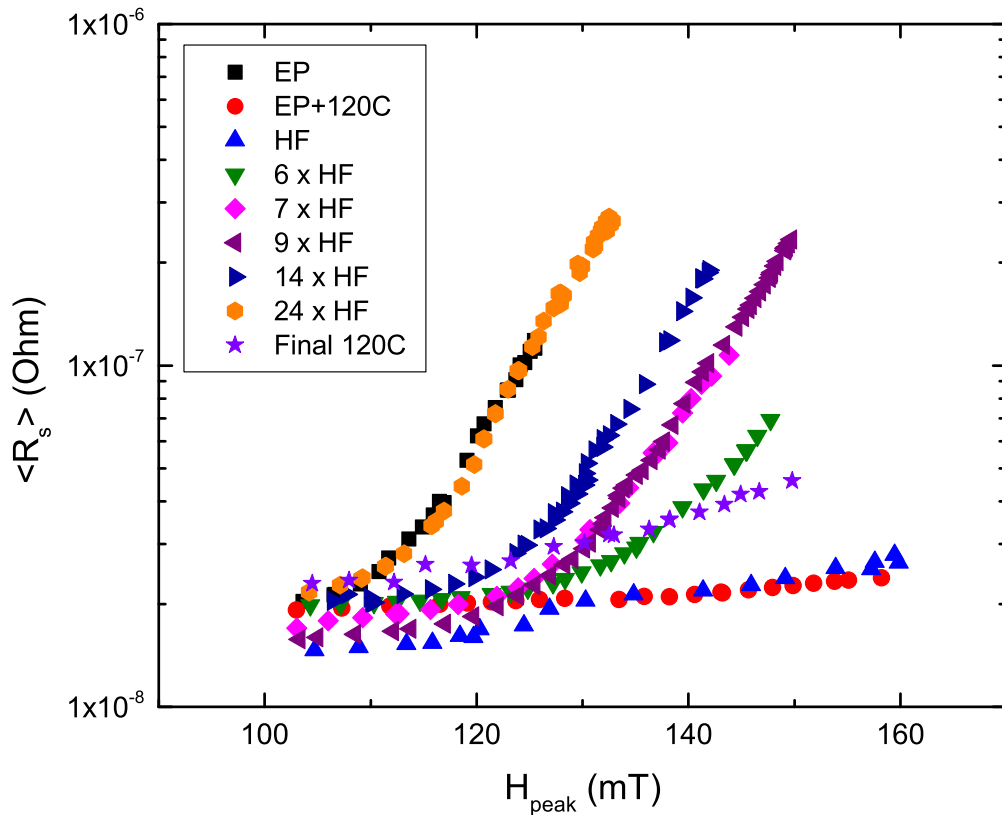


FIG. 9. Evolution of the high field Q-slope with multiple HF rinse cycles for the electropolished cavity TE1ACC005. Notice gradual emergence of the high field Q-slope as more and more niobium is consumed.

consumed) the HFQS is present, but the onset field is higher than before 120°C bake. Subsequent HF rinses make the onset field lower and lower until after 24 HF rinse cycles (\approx 36-48 nm of niobium consumed) $Q_0(H_{\text{peak}})$ curve is essentially back to the pre-baking

shape. Therefore the required material removal to completely cancel the effect of mild baking on the HFQS is between 14 and 24 HF rinses or in terms of thickness approximately 21-48 nanometers. It is in a reasonable agreement with the results of Ereemeev [3] and Ciovati [4].

Recently we proposed a model [19] for the HFQS based on the small normal conducting hydrides within the penetration depth, which are superconducting by proximity effect up to the HFQS onset field. In brief, we suggested that all the cavities have a significant hydrogen concentration in the near-surface layer. Accompanying such a concentration may be a layer of superabundant vacancy-hydrogen complexes with the concentrations of order a few 10^{-3} at.%. Upon cooldown to 2 K interstitial near-surface hydrogen can form hydrides with vacancy-hydrogen complexes serving as nucleation centers. These small hydrides can be superconducting by proximity effect up to the critical field $H_b \sim 1/d$, where d is the hydride characteristic size. Mild baking effect is explained by the dissociation and removal of Vac-H complexes thus providing much fewer sites for hydride nucleation. The following form for $R_s(H)$ was proposed based on this mechanism:

$$R_s(H) \approx R_0 + A \cdot F_H(H, \mu, \sigma) = R_0 + A \frac{1}{2} \left[1 - \operatorname{erf} \left(\frac{\frac{1}{H} - \frac{1}{H_0}}{\sqrt{2\sigma^2}} \right) \right] \quad (4)$$

where R_0 is the surface resistance below the HFQS onset, $A \sim \sigma_n R_n$ - constant dependent on the surface density of hydrides and their surface resistance in the normal state, and F_H is the cumulative distribution function of the distribution of $1/d$ corresponding to the range of critical fields of the precipitates with the normal distribution of their diameters. We found that the shape of the $Q(H)$ curve in the HFQS regime for all the cavities we studied can be fitted very well by such model.

IV. CONCLUSIONS

We have studied the near-surface structure of mild baked SRF niobium cavities via material nanoremoval followed by RF testing. $Q_0(H_{\text{peak}})$ curves, residual and BCS surface resistances, gap value, and electron mean free path for different material removal thicknesses were obtained. A simple way to improve the quality factor based on hydrofluoric acid rinse was developed for practical applications. The low field Q-slope was found to be

governed by the material structure within about 6 nanometers. Furthermore, the LFQS was found to be consistent in most cases with the inverse quadratic field dependence, which may be a signature of additional constant with field RF losses. Both medium and high field Q-slopes were found to be affected primarily by the material thickness of about 20-50 nanometers thick. MFQS was best fitted by the linear dependence of the surface resistance on field emphasizing possible roles of hydrides and strong links. HFQS was found to gradually re-emerge with the thickness of the removed material and the depth of the mild baking effect on HFQS was found to be in agreement with previous studies.

V. ACKNOWLEDGEMENTS

Authors would like to acknowledge Hasan Padamsee for suggesting the experiment and reading the manuscript, Charlie Cooper for tumbling one of the cavities, Dmitri Sergatskov for help with cavity tests, and Damon Bice and Allan Rowe for cavity processing. The work was partially supported by the DOE Office of Nuclear Physics. Fermilab is operated by Fermi Research Alliance, LLC under Contract No. DE-AC02-07CH11359 with the United States Department of Energy.

-
- [1] H. Padamsee, *RF Superconductivity: Volume II: Science, Technology and Applications; Chapters 3, 5* (Wiley-VCH, 2009).
 - [2] P. Kneisel, in *Proceedings of the 1999 Workshop on RF Superconductivity*, TuP044 (1999).
 - [3] G. Eremeev and H. Padamsee, *Physica C*, **441**, 134 (2006).
 - [4] G. Ciovati, P. Kneisel, and A. Gurevich, *Phys. Rev. ST Accel. Beams*, **10**, 062002 (2007).
 - [5] G. Ciovati, JLAB-TN-03-003.
 - [6] J. Halbritter, Tech. Rep. FZK 3/70-6 (Forschungszentrum Karlsruhe, 1970).
 - [7] G. Ciovati, in *Proceedings of Workshop on Pushing the Limits of RF Superconductivity* (2004) p. 52.
 - [8] G. Ciovati, *J. Appl. Phys.*, **96**, 1591 (2004).
 - [9] J. Halbritter, in *Proceedings of the 38th Eloisitron Workshop* (1999) p. 59.
 - [10] W. Weingarten, *Phys. Rev. ST Accel. Beams*, **14**, 101002 (2011).

- [11] V. Palmieri, in *Proceedings of the 12th Workshop on RF Superconductivity* (2005) p. 162.
- [12] J. Halbritter, P. Kneisel, and K. Saito, in *Proceedings of the 6th Workshop on RF Superconductivity* (1993) pp. 617–627.
- [13] J. Halbritter, *J. Appl. Phys.*, **97**, 083904 (2005).
- [14] A. Gurevich, *Physica C*, **441**, 38 (2006).
- [15] A. Romanenko, J. P. Ozelis, A. Grassellino, and H. Padamsee, in *Proceedings of IPAC'12, WEPPC116* (2012).
- [16] B. Visentin, in *Proceedings of the 11th Workshop on RF Superconductivity*, TuO01 (2003).
- [17] G. Ciovati, in *Proceedings of the 13th Workshop on RF Superconductivity* (2007) p. 70.
- [18] G. Ciovati, G. Myneni, F. Stevie, P. Maheshwari, and D. Griffis, *Phys. Rev. ST Accel. Beams*, **13**, 022002 (2010).
- [19] A. Romanenko, F. Barkov, L. D. Cooley, and A. Grassellino, “Proximity breakdown of hydrides in superconducting niobium cavities,” FERMILAB-PUB-12-427-TD.